Modelling Viscoelastic Creep Response of Porcine Lumbar Spinal Units Exposed to Repeated Flexion-Compression Loading

Concetta F. Morino, Shea T. Middleton, Elizabeth Dimbath, Joost Op 't Eynde, Jason Kait, Cameron R. 'Dale' Bass

Abstract

Lower back pain is highly prevalent globally, yet the aetiology is poorly and incompletely understood. Lower back pain is common among those with a history of frequent cyclic combined loading, such as long-haul and short-haul truck drivers and high-speed watercraft operators. Characterization of the viscoelastic behaviour of the lumbar spine will improve understanding of lower back pain, provide data for computational models of the lumbar spine, and inform injury prediction models. Ten osteoligamentous porcine functional spinal units were mechanically tested until primary soft tissue failure using a cyclic combined flexion-compression loading profile. Displacement and force data were then fit to a quasilinear viscoelastic model with two time constants (24.6s and 575s), three creep coefficients, and two instantaneous elastic parameters. Results indicated a very good fit from experimental data to model data (R^2 = 0.997 ± 0.003), largely dominated by the steady-state and slow rate creep coefficients. Quasilinear viscoelastic (QLV) modelling appears to be a suitable method for modelling porcine lumbar spine viscoelastic behaviour.

Keywords Combined loading, creep behaviour, lumbar spine, mathematical model, quasilinear viscoelasticity

I. INTRODUCTION

Lower back pain (LBP) is a common condition that affects 50-80% of adults worldwide during their lifetime [1]. United States (US) military service personnel are particularly vulnerable to LBP, with an incidence rate of 40.5 per 1000 person-years [2]. Furthermore, military vehicle service operators have an increased risk of LBP with a rate of 54.2 per 1000 person-years [3]. Although LBP is prevalent, the aetiology of injury that leads to chronic pain is not well understood. In 85-90% of cases, patients are not diagnosed with a specific pathoanatomical origin of LBP [4]. However, it has been established that differing spinal loading configuration is related to long-term creep response. Prolonged lumbar flexion, present in a seated posture, can lead to vertebral disc damage under even low load levels [5]. Compression, particularly when coincident with flexion in cyclic combined loading scenarios, is also associated with lumbar spine degeneration [6]. Following, those regularly exposed to prolonged flexion and compression, such as helicopter pilots and high-speed watercraft occupants, are at increased risk of lumbar spine degeneration [7-10]. Autonomous vehicles also present new challenges when considering loading during transportation. They allow for varied seating postures compared to those found in typical automobiles, and thus present possible different spinal loading configurations [11,12]. It has been established that loading characteristics of the spine differ among those who suffer from LBP, and repetitive and/or heavy mechanical loading or bending scenarios are associated with increased prevalence of LBP [13,14].

The lumbar spine exhibits viscoelastic creep behaviour in static and cyclic loading conditions [6,15]. To better characterise lumbar spine behavior due to cyclic loading, viscoelastic response behaviour must be determined. Studies have been performed that examine the viscoelastic response of the human spine. Reference [16] observed stress-relaxation in human L4L5 vertebral discs in tension, noting that the large amount of water content in the disc is strongly related to the viscoelastic behavior. Reference [17] examined the dynamic characteristics of viscoelastic behavior in the nucleus pulposus when subject to shear deformation. Efforts have also been made to examine the viscoelastic behavior of the ligaments associated with the lumbar spine. Computational mechanical response models use parameters derived from observing viscoelastic response to inform simulations [18]. Soft tissue dynamic responses of human and porcine ligaments associated with the lumbar spine have been modelled in prior research [15,19,20]. Reference [21] investigated viscoelastic properties of cervical spine ligaments subject to high strain rate deformation. Reference [18] characterised the temperature-dependent viscoelasticity of porcine anterior longitudinal ligaments. Reference [22] described viscoelastic characteristics of human lumbar spines subjected to flexion during prolonged stooping. Primary creep, characterized by transient fast-rate creep that precedes steady-state creep and occurs after instantaneous deformation, is relevant to examine as the necessary precursor for more injurious secondary and tertiary creep

states. This has been evidenced by an assertion that primary creep contributes to the amplitude of further creep in the pubic symphysis, which is a similar cartilaginous disc to the intervertebral discs [23]. Cadaveric human lumbar spine testing under static compressive loads also revealed the importance of the strain rate characteristics directly proceeding instantaneous deformation, represented by primary creep, when considering disc degeneration [24].

Despite the quadrupedal posture of a pig, it has been shown that the loading configuration and ligament behavior is similar between the human and porcine lumbar spine [18,25,26]. Consistent loading direction and similar structural and anatomical characteristics make the porcine lumbar spine a valid animal surrogate for the human lumbar spine [25,27]. Particularly, other studies have used the porcine lumbar spine as an analog for the human lumbar spine due to the similarities in anatomy, mechanical properties, and dynamic behaviour [25,28-31]. Moreover, the porcine vertebral disc has been shown to exhibit similar disc degeneration and cell response to external stimuli when compared to a human [32,33].

However, there is a lack of study regarding the viscoelastic responses of complete porcine lumbar spinal segments, incorporating all the osteoligamentous components, particularly in cyclic loading scenarios. The purpose of this study is to model the complex viscoelastic nature of the lumbar spine by fitting a mathematical model to experimental data of porcine lumbar spinal units subject to cyclic flexion-compression loading. Since the fundamental viscoelasticity of the lumbar spine transmits forces both above and below the lumbar region, the results of this study will improve our understanding of lumbar spine biomechanics and provide valuable short and long term data for viscoelastic computational modelling.

II. METHODS

Mechanical Testing

Ten porcine osteoligamentous lumbar functional spinal units (FSUs) from six female Yorkshire pigs (average mass = 65 kg) were loaded in combined cyclic flexion and cyclic compression until failure was observed. Each frozen-thawed specimen consisted of two adjacent lumbar vertebral bodies and the intervertebral disc (IVD) between them. Extraneous musculature was removed for disc and vertebral body visibility but the osteoligamentous spine was retained. Three screws were fixed in each exterior endplate along with two 0.078" stainless steel Kirschner wires into the distal regions of both vertebral bodies. Screws and wire were then covered by polymethyl methacrylate (PMMA) and both ends cast into aluminum pots with urethane casting resin (R1 Fast Cast® #891, Goldenwest Mfg, Inc., Grass Valley, CA). This specimen preparation process allowed for the application of compression and flexion to the FSU without direct contact with the IVD or endplates. Intervertebral disc heights and endplate areas were measured from pre-test images obtained with a Nikon XTH 225 ST high resolution X-ray microcomputed tomography (MicroCT) scanner and processed using Fiji image processing software [34]. High-resolution MicroCT was also used post-test to assess specimens for damage to the disc that was not present in the pre-test scans. Specimen characteristics were as follows:

TABLE I
TEST CHARACTERISTIC INFORMATION FOR EACH SPECIMEN

Test Number	Pig number	Disc location	Disc height (mm)	Average endplate area (mm^2)	Peak applied load (N)	Test duration until inflection (s)
Test 1	1	L2L3	3.57	481	2000	990
Test 2	1	L4L5	3.32	508	2300	170
Test 3	2	L1L2	3.81	529	1700	260
Test 4	2	L3L4	3.78	584	1700	340
Test 5	2	L5L6	4.00	603	2300	240
Test 6	3	TXL1	4.34	592	2300	390
Test 7	4	L3L4	3.12	486	1400	120
Test 8	4	L1L2	2.84	460	600	190
Test 9	5	L2L2	3.55	584	1200	165
Test 10	6	L3L4	4.23	667	1400	140
Mean	-		3.66 ± 0.45	549 ± 63	1690 ± 530	300 ± 244

Specimens were secured in a biaxial servohydraulic test machine with independent flexion and compression actuators (MTS, Eden Prairie, MN, USA). A linear variable differential transformer (LVDT) measured linear

displacement and two load cells (AMTI MC5-6-500 and Denton 1716A) recorded applied forces and bending moments. The superior end of the FSU was rigidly fixed to the rotational actuator while the inferior end was in contact with the axial compression actuator, while free to translate on ball bearings in the x-y plane. Mechanical testing occurred in an environmental chamber surrounding the test area to maintain relevant physiological temperature (37 °C) and nearly 100% humidity.

Axial cyclic compression was applied at 1 Hz and offset cyclic flexion was applied at 1 Hz as a ramp from 0° to 6°. The applied combined loading profile, shown in Figure 1 was modelled after repeated loading experienced by high-speed planing boat operators [10]. Typical boat motions produce vertical underbody compressive loads every 1-3 seconds. Watercraft pitch and compression combine to produce lumbar flexion with offset flexion from the peak compression. The minimum load of the sinusoidal compression was 76 N, which represents minimum compression due to human upper body mass, scaled down to porcine endplate area. The peak load varied from 600 N – 2,300 N depending on the test. Values for peak loads were chosen to establish a range of compressive loads below the threshold of endplate failure in cyclic loading [35]. The data utilised for mathematical modelling in this study was bound by the 'start' of loading and the inflection in the slope of the displacement-logtime history, denoting the end of primary creep. The 'start' of loading excluded the compression ramp before specified compression was reached and any initial time that included filtering artifacts in the first 0-60s. Specimens were loaded until shortly after this inflection to prevent injury.

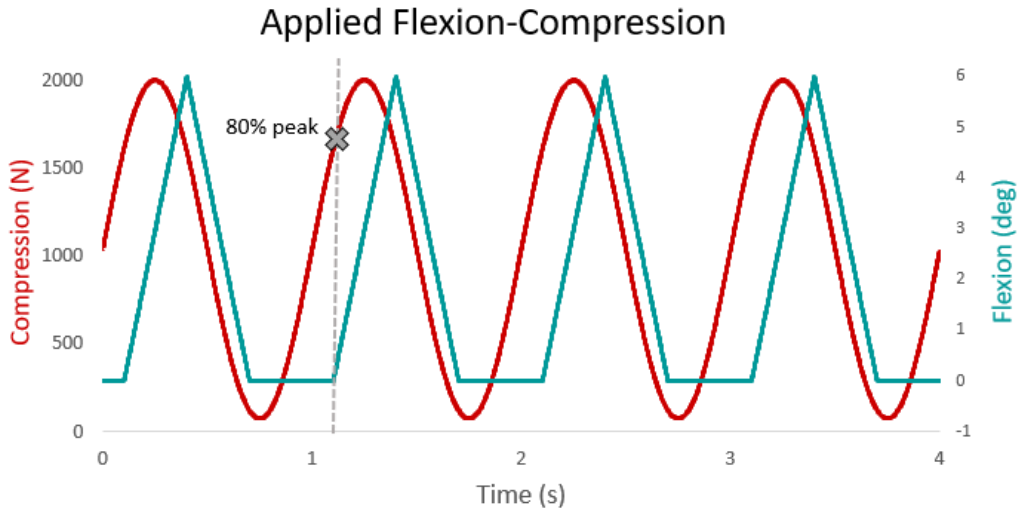

Fig. 1. Applied loading profile of sinusoidal compression at 1 Hz with a peak load of 2000 N and offset ramped flexion at 1 Hz, modelling idealised exposures seen by high speed water-planing boat operators [36]. Flexion and compression values differed per test.

Mathematical Modelling

Creep analysis assumed quasilinear viscoelasticity (QLV) in which the time dependence (viscoelastic creep) and displacement dependence (instantaneous elastic behaviour) are separable. Previous viscoelasticity studies of the spine have indicated this to be a valid assumption for relaxation response in some osteoligamentous biological materials [20,21,37]. Quasilinear viscoelastic models have previously been used to model stress-relaxation in human cervical spine IVDs exposed to high-rate indentation tests and to cyclic compression as well as ovine cervical spine IVDs undergoing tension [38,39]. Assuming the quasilinear reciprocity holds between creep and relaxation, QLV should also be appropriate for creep response of the same or similar materials [21,40,41]. Creep response was determined using a generalised Kelvin-Voigt model, with two time constants (τ_i) and creep coefficients (J_i) as well as a steady-state creep coefficient (J_0). The nonlinear instantaneous elastic response was modelled as a Fung exponential form with two instantaneous elastic parameters (A, B) [21]. The instantaneous elastic displacement function is

$$\delta^e(t) = \frac{1}{A}\ln\left(\frac{F(t)}{B} + 1\right) \tag{1}$$

The Boltzmann history integral for displacement due to applied stress is,

$$\delta(t) = \int_0^t J(t-\tau)\frac{\partial \delta^e[F(\theta)]}{\partial \theta} d\theta \tag{2}$$

where J is a creep constant, δ is the displacement, and F is the instantaneous force. The creep function, J(t), is

$$J(t) = J_0 + \sum_{i=1}^{n} J_i(1 - e^{-\beta_i t}) \quad (3)$$

where $J_0 + \Sigma J_i = 1$, $J_i \geq 0$, and $\beta_i \geq 0$. Thus, the instantaneous displacement is

$$\delta(t) = \delta_0(t) + \sum_{i=1}^{n} \delta_i(t) \quad (4)$$

which can be decomposed to:

$$\delta_0(t) = J_0 \int_0^t \frac{\partial \delta^e[F(\theta)]}{\partial \theta} d\theta \quad (5)$$

$$\delta_i(t) = J_i \int_0^t \frac{\left(1 - e^{-\beta_i(t-\theta)}\right)\partial \delta^e[F(\theta)]}{\partial \theta} d\theta \quad (6)$$

Axial displacement data and normal-direction force data were used to analyse specimen creep. Inflections in primary creep were determined based on deviation of the force displacement history from a loglinear trendline. Data before inflection were analysed in Microsoft Excel using iterative optimisation. All datasets were downsampled to approximately 50,000 points to improve optimisation efficiency. One dataset was analysed with the model without downsampling and indicated no substantial difference in outputs. Displacement data was filtered with an 8th order phaseless low-pass Butterworth filter with a 0.1 Hz cutoff frequency to smooth data oscillations for slope assessments.

To create a general optimisation, all ten creep responses were constrained to have the same time constants (τ_1 and τ_2) and creep constants (J_1, J_2, J_0). These constants were averaged to exhibit the assumption that a creep behavior model is qualitatively similar with the same time constants even with different specimens. The instantaneous elastic response parameters A and B were optimised individually based on each test due to differences in displacement. The optimisation process was run multiple times with different A, B, and constant values to determine sensitivity. The solver optimised for the combined minimum sum of squares error (SSE) of the entire dataset. R^2 was also assessed as a measure of model fit.

III. RESULTS

Ten osteoligamentous FSUs from six pigs were analysed to characterise viscoelastic properties. No disc damage was observed in pre- or post- test MicroCT images. The quasilinear viscoelastic model provided a good fit for each test where the average SSE value is 0.478 ± 0.454 and the average R^2 value is 0.997 ± 0.003 (full list of R^2 and SSE values in Appendix). Repeated optimisations with differing initial parameters converged to very similar final values. Figure 2 illustrates a comparison of the displacement versus time curve of Test 4 for experimental data and the fitted model. The R^2 value associated with this fit is greater than 0.999.

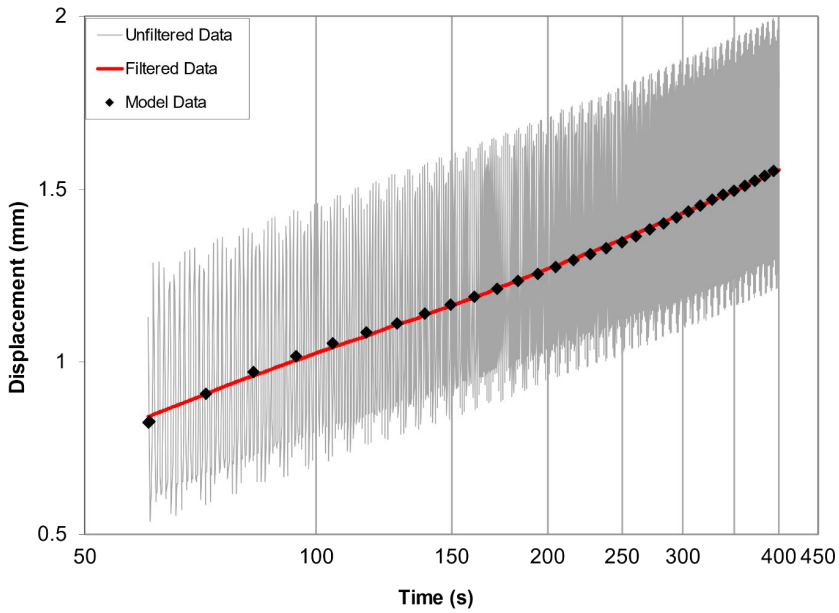

Fig. 2. Displacement versus time for Test 4, with original oscillatory displacement, filtered displacement input, and model displacement shown.

The average full test time was 8,770 ± 8,910 seconds. Full displacement changes in analysed data portions ranged from 0.260mm to 1.238mm (average 0.710 ± 0.320 mm). The average test duration before primary inflection was 300 ± 244 seconds, indicating that primary creep inflection tends to happen early in the test. The exact point of inflection in each test does have a degree of subjectivity to it; typical second-derivative zero-crossing inflection determination methods were not applicable due to oscillation of datapoints. However, the results were not sensitive to exact inflection point determination.

Independently optimised parameters were comparable across specimens, but some values were different based on initial estimates, timescale, and size of the test. Time constants were optimised to be τ_1 = 24.6s and τ_2 = 575s. Creep parameters were optimised so that the steady state coefficient J_0 = 0.500 and the two rate-dependent creep constants were J_1 = 0.198 and J_2 = 0.302. Thus, the steady state coefficient contributed the most to creep behaviour in each test, accounting for 50% of the behavior, while J_2 contributed the second most to the overall creep behaviour.

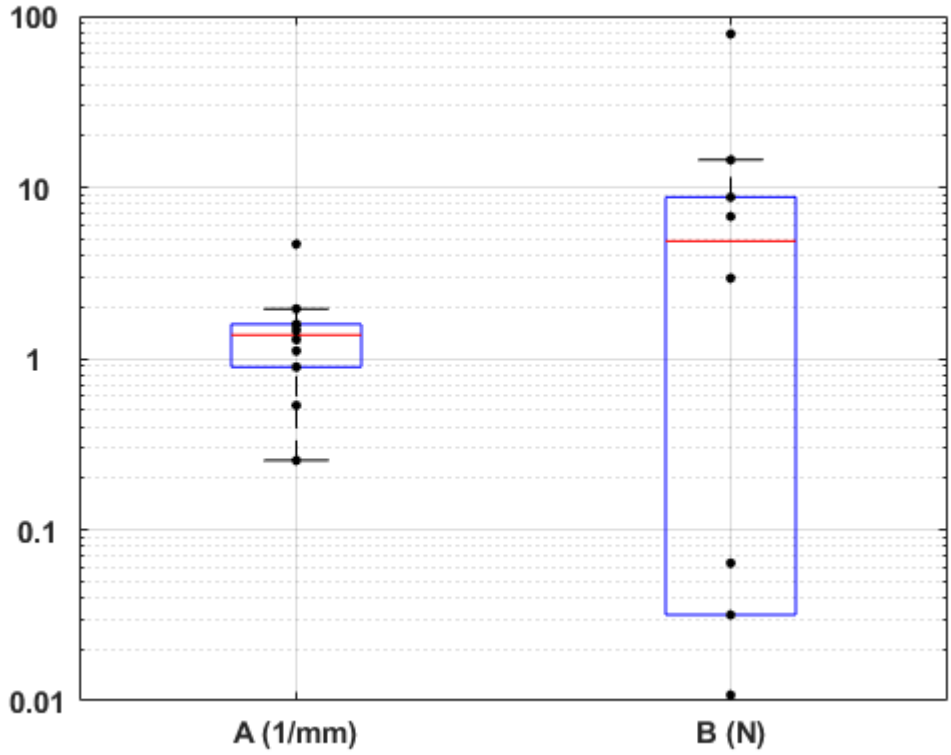

Fig. 3. Box plot displaying the values for parameters A (left) and B (right) for all tests (n=10).

Instantaneous elastic response parameters A and B both showed substantial deviation among tests with parameter A ranging from 0.254 to 4.653 mm^{-1} and parameter B ranging from 1.23 x 10^{-6} to 78.62 N (Figure3). However, the high range of these values is due to outliers, as shown in Figure 3. The median value for A is 1.373 mm^{-1} with an interquartile range (IQR) of 0.633 mm^{-1} and the median value for B is 4.844 N with an interquartile range of 8.724 N. The values of the instantaneous elastic response using test-specific A and B values and arbitrary stress values ranging from 0 to 2.3 kNs are shown in Figure 4. This figure shows that there is still considerable variation in instantaneous response between tests.

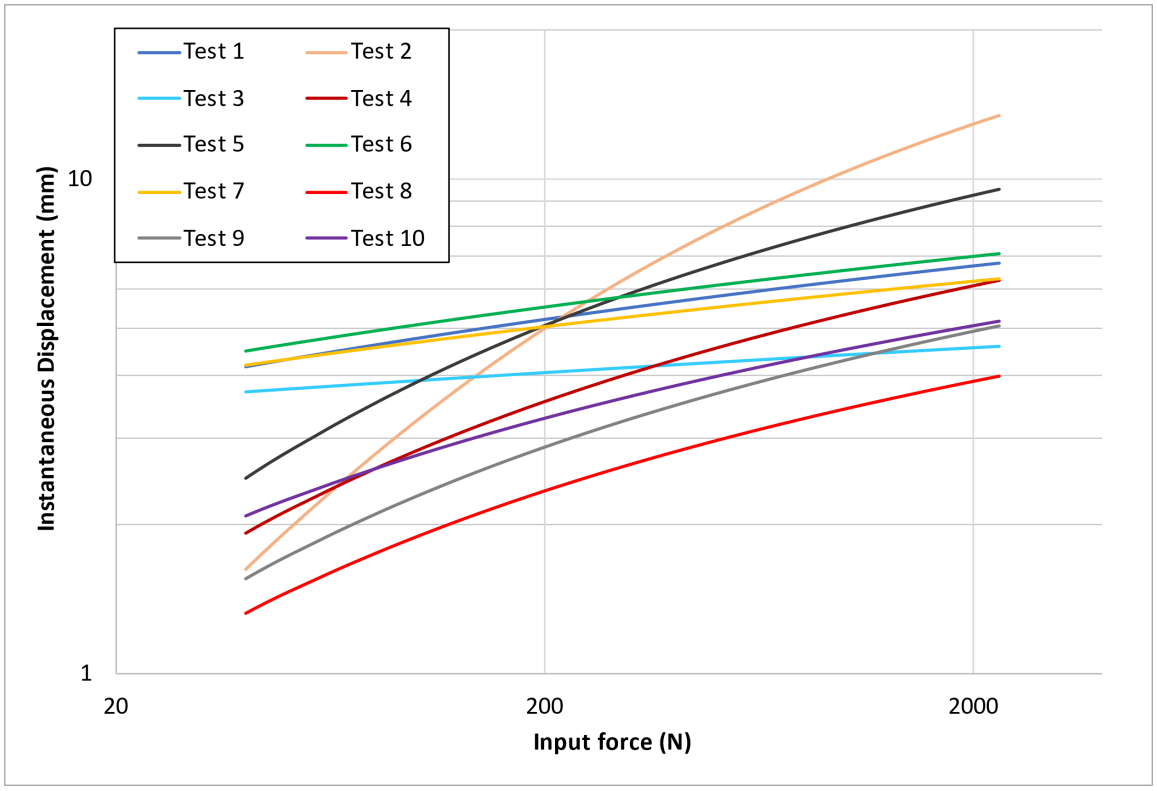

Fig. 4. Calculated instantaneous elastic response for ten pairs of A and B parameters with arbitrary force input of 0-2.3kN.

For qualitative comparison of curve shapes, Figure 5 shows the normalised time versus normalised model displacement between 0 and 1 for each of the 10 models created. Figure 6 in the Appendix shows the non-normalised curves. The oscillating nature of some of the curves is due to the cyclic force waveform.

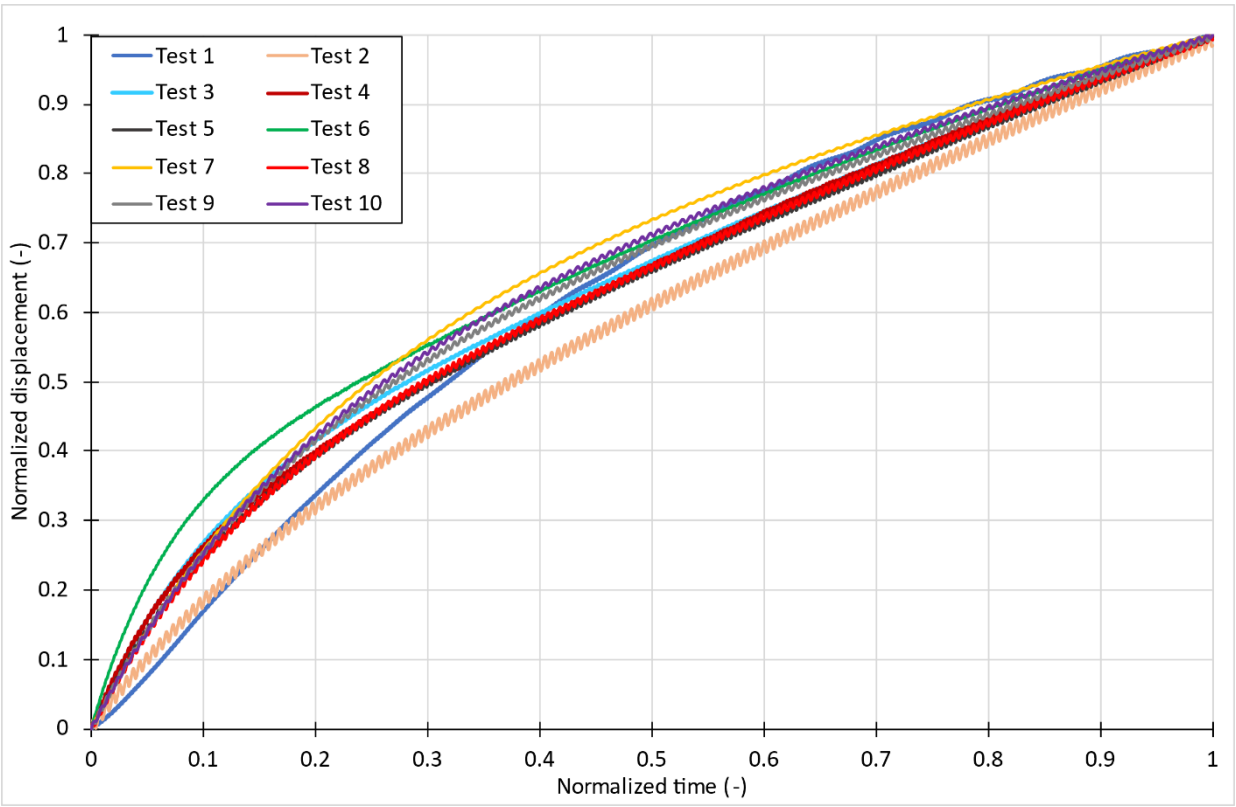

Fig. 5. Normalised time versus normalised model displacement for all models. Normalised values are $\frac{value-min}{max-min}$.

IV. DISCUSSION

Viscoelastic behaviour of the creep response of lumbar FSUs subject to cyclic combined loading is examined in this study. This is the first study to characterise long-duration cyclic creep in combined loading in porcine lumbar spinal units. Ten tests were performed and analysed with cyclic combined loading conditions and similar loading configurations. Results from these tests can be used to investigate the creep response associated with cyclic lumbar spine loading, to provide structural characterization to support *in vivo* tests with live pigs, and to develop a creep model that is capable of comparing the primary creep responses *in vitro* of porcine and human lumbar spines for the purpose of interspecies scaling.

Viscoelastic material characterization is important for biofidelic modelling. It is pertinent to model a wide range of loading scenarios, from typical posture when driving an automobile to the high-frequency combined loading present in high-speed watercraft, to fully understand the capabilities and vulnerabilities of the spine and other body components for long-duration and short duration loading. For example, it is unknown whether long-term creep increases the risk of lumbar spinal injuries by pre-compressing the relative position of endplates, exacerbating injury risk in impact loading. Variety in modelling is particularly relevant as new advances in transportation are made through the increasing utilisation of autonomous vehicles. Autonomous vehicles offer a much wider range of seating variation and thus present a new challenge in preventing spinal injuries; current safety standards typically only account for upright, front-facing passengers. Posture in autonomous vehicles often differs compared to standard automobile seated positions [11]. This may introduce the spine to different loading configurations and thus new injury risks in impact or regular use [12,42]. The data presented in this study exhibit the differences in creep response in different loading configurations based on magnitude of applied force.

The creep models presented in this study show good fit with the measured data: the average SSE value is 0.478 ± 0.454 and the average R^2 value is 0.997 ± 0.003. The SSE analysis was conducted over an average of 3,010 ± 1,160 datapoints per test, so an SSE value of less than 1 shows a very good fit. All tests showed a roughly logarithmic increase in displacement until reaching an initial inflection point, as is typical for characterisations of primary creep. The similarity in shape of these time versus displacement curves (Fig. 5) for ten different tests, and the capability for all ten tests to fit to the same creep constants with low SSE values, indicates the goodness of fit of the model to general viscoelastic behaviour of porcine lumbar FSUs subject to combined flexion and compression.

Test results revealed a large amount of variation in instantaneous displacement values A and B. Initial displacement is sometimes poorly represented by the model while long-term displacement is more consistently predicted. We believe that this is primarily due to initial variation in disc height and endplate area that was not properly accounted for while modeling. Endplate area can be measured using pre-test MicroCT images of the FSUs, which can then be used to convert force to stress; this is likely to be highly relevant. For instance, the stress in Test 2 is about 4.53 MPa, while the stress in Test 5 is 3.81 MPa, despite having the same force magnitude of 2300N. In future modeling efforts, including stress-strain values will potentially decrease interspecimen variation and account for relevant individual anatomical data.

In the creep response estimation function, the steady state coefficient J_0 dominates in each model with little variance. The second largest coefficient was the long strain-rate coefficient, J_2 (associated with timescale τ_2 = 575 s); combined with the steady-state coefficients J_0, these two constants account for 80% of the creep behaviour while the fast-rate constant J_1 only accounts for about 20%. This may indicate that creep could be accurately modelled using only one creep constant and associated time constant as well as a steady state creep constant, because the effects of the long time constant are negligible for tests with a short time frame. However, the overestimation of the share of J_2 may also be related to Test 1, which is substantially longer than the other tests (1,000s versus 120s to 390s); removing this test may improve model fit and distribute creep constants more evenly, but will result in the model losing the versatility to work with longer primary creep sections more typical of loading over many hours of standing or seated posture.

Reference [20] examined ligaments in the cervical spine with a similar QLV model for relaxation after high strain rate input and reported averages that ranged between 0.61-0.69 and 0.19-0.25 for the fast rate coefficient and steady state coefficient, respectively, when considering the anterior longitudinal ligament, posterior longitudinal ligament, and ligamentum flavum. This model had used four time constants with decade values (1 s, 100 ms, 10 ms, and 1 ms) compared to our two time constants [20]. These decade values, however, appear to be non-specific to the tested material, while ours were optimised for the dataset. The same group also examined faster strain-

rate deformations in cervical spine ligaments and reported fast rate and steady state coefficients ranging from 0.65-0.76 and 0.15-0.31, respectively [21]. In both cases, we see a substantially lower fast rate coefficient (J_1 = 0.198) and substantially higher steady state creep coefficient (J_0 = 0.500) [20,21]. As our study examines the entire FSU, this could account for the difference when compared to the viscoelastic behavior exhibited by ligaments.

While the porcine lumbar spine has shown to be a valid animal model, there are also inherent differences between human and porcine spines that support the need to scale these results for future comparison to human lumbar spine creep data. Reference [26] establishes that the range of motion in each separated porcine lumbar FSU is typically lower than that of a human when subject to combined flexion/extension but generally comparable when subject to lateral bending or axial rotation. Reference [43], however, showed that the pig had significantly increased range of motion when considering the entire lumbar spine in flexion/extension, lateral bending, and axial rotation scenarios. These findings indicate that the porcine lumbar spine may be stiffer than the human spine when considering individual FSUs but may be less stiff overall. Reference [25] compares anatomical measurements of pig vertebrae to 50% male vertebrae, determining that in the lumbar spine the porcine vertebral width was on average 40% smaller and the porcine vertebral body depth was on average 30% smaller than the human. The average porcine mass in this study (65kg) is even smaller than the average from that study (80.7kg) so efforts must be made to scale accordingly for comparison [25]. As viscoelasticity and morphology are interrelated by stress and strain, maintaining a consistent scaling metric allows for better viscoelastic comparison between human and pig.

This study is not without limitations. First, a larger sample size could further improve the accuracy of the creep constants and minimise variation. Averaging the time and creep constants likely contributed to this variation as well. Exact numbers for specific creep and instantaneous elastic values varied based on initial inputs to the iterative solver, indicating that the model is not particularly sensitive to any one variable; however, the same trends regarding which creep constants were the largest always persisted. Further, while the R^2 or SSE show great model fit, a large number of data points, such as the case in this study, can inflate the accuracy interpretation. Future efforts may include cross-validation of R^2 and SSE values when the dataset is segmented into consistently sized sections. The method for determining data inflection could also be improved by developing and imposing an objective, robust, and reduced noise computational algorithm to accurately locate second derivative-based inflections.

V. CONCLUSIONS

This study is the first to mathematically model the primary creep behaviour of porcine lumbar spine subject to cyclic combined flexion-compression loading. The porcine lumbar spine exhibits substantial viscoelastic creep behaviour over timescales from seconds to minutes. The model provides a good fit to 10 different experimental datasets of primary creep in lumbar spine. The only two test-specific parameters in the model are instantaneous elastic response (median A = 1.373 mm^{-1} with IQR = 0.633 mm^{-1}, median B = 4.844 N with IQR = 8.724 N), and the other five parameters (τ_1 = 24.6s, τ_2 = 575s, J_1 = 0.198, J_2 = 0.302, J_0 = 0.500) were optimised and consistent for the whole dataset. This study reasonably characterises viscoelastic creep effects on a lumbar functional spinal unit. This information can be used to better inform the creep response caused in cyclic loading similar to those experienced by high-speed watercraft or helicopter operators.

VI. ACKNOWLEDGEMENT

The authors gratefully acknowledge the funding and collaboration from MTEC Prime Award W81XWH-15-9-0001, subcontract MTEC (Medical Technology Enterprise Consortium)-18-04-I-PREDICT (Incapacitation Prediction for Readiness in Expeditionary Domains: an Integrated Computational Tool) -07.

VII. REFERENCES

[1] James, S.L., Abate, D., et al. Global, regional, and national incidence, prevalence, and years lived with disability for 354 diseases and injuries for 195 countries and territories, 1990–2017: a systematic analysis for the Global Burden of Disease Study 2017. *The Lancet*, 2018. 392(10159): p. 1789-1858

[2] Knox, J., Orchowski, J., et al. The Incidence of Low Back Pain in Active Duty United States Military Service Members. *Spine*, 2011. 36(18): p. 1492

[3] Knox, J.B., Orchowski, J.R., et al. Occupational driving as a risk factor for low back pain in active-duty military service members. *The Spine Journal*, 2014. 14(4): p. 592-597

[4] Finucane, L.M., Downie, A., et al. International Framework for Red Flags for Potential Serious Spinal Pathologies. *Journal of Orthopaedic & Sports Physical Therapy*, 2020. 50(7): p. 350-372

[5] Adams, M.A. and Hutton, W.C. The effect of posture on the lumbar spine. *The Journal of Bone & Joint Surgery British Volume*, 1985. 67-B(4): p. 625-629

[6] Yoganandan, N., Cusick, J.F., Pintar, F.A., Droese, K., and Reinartz, J. Cyclic Compression-Flexion Loading of the Human Lumbar Spine. *Spine*, 1994. 19(7): p. 784

[7] Landau, D.-A., Chapnick, L., et al. Cervical and lumbar MRI findings in aviators as a function of aircraft type. *Aviation, Space, and Environmental Medicine*, 2006. 77(11): p. 1158-1161

[8] Kåsin, J.I., Mansfield, N., and Wagstaff, A. Whole body vibration in helicopters: risk assessment in relation to low back pain. *Aviation, Space, and Environmental Medicine*, 2011. 82(8): p. 790-796

[9] Knox, J.B., Deal, J.B., and Knox, J.A. Lumbar Disc Herniation in Military Helicopter Pilots vs. Matched Controls. *Aerospace Medicine and Human Performance*, 2018. 89(5): p. 442-445

[10] Bass, D., Salzar, R., Ziemba, A., Lucas, S., and Peterson, R. The Modeling and Measurement of Humans in High Speed Planing Boats under Repeated Vertical Impacts. 2005

[11] Hong-yan, W., Ming-ming, Z., Georges, B., and Xu-guang, W. Automobile Driver Posture Monitoring Systems: A Review. 2019

[12] Humm, J., Yoganandan, N., et al. A novel posture control device to induce high-rate complex loads for spine biomechanical studies. *Journal of Biomechanics*, 2021. 123: p. 110537

[13] Marras, W.S., Davis, K.G., Ferguson, S.A., Lucas, B.R., and Gupta, P. Spine Loading Characteristics of Patients With Low Back Pain Compared With Asymptomatic Individuals:. *Spine*, 2001. 26(23): p. 2566-2574

[14] Bakker, E.W.P., Verhagen, A.P., van Trijffel, E., Lucas, C., and Koes, B.W. Spinal Mechanical Load as a Risk Factor for Low Back Pain: A Systematic Review of Prospective Cohort Studies. *Spine*, 2009. 34(8): p. E281

[15] Little, J.S. and Khalsa, P.S. Human Lumbar Spine Creep during Cyclic and Static Flexion: Creep Rate, Biomechanics, and Facet Joint Capsule Strain. *Annals of Biomedical Engineering*, 2005. 33(3): p. 391-401

[16] Panagiotacopulos, N.D., Pope, M.H., Bloch, R., and Krag, M.H. Water content in human intervertebral discs: part II. viscoelastic behavior. *Spine*, 1987. 12(9): p. 918-924

[17] Iatridis, J.C., Weidenbaum, M., Setton, L.A., and Mow, V.C. Is the Nucleus Pulposus a Solid or a Fluid? Mechanical Behaviors of the Nucleus Pulposus of the Human Intervertebral Disc. *Spine*, 1996. 21(10): p. 1174-1184

[18] Bass, C.R., Planchak, C.J., et al. The Temperature-Dependent Viscoelasticity of Porcine Lumbar Spine Ligaments:. *Spine*, 2007. 32(16): p. E436-E442

[19] Yoganandan, N., Pintar, F., et al. Dynamic response of human cervical spine ligaments. *Spine*, 1989. 14(10): p. 1102-1110

[20] Lucas, S.R., Bass, C.R., et al. Viscoelastic and failure properties of spine ligament collagen fascicles. *Biomechanics and Modeling in Mechanobiology*, 2009. 8(6): p. 487-498

[21] Lucas, S.R., Bass, C.R., et al. Viscoelastic properties of the cervical spinal ligaments under fast strain-rate deformations. *Acta Biomaterialia*, 2008. 4(1): p. 117-125

[22] Shin, G., Mirka, G.A., and Loboa, E.G. Viscoelastic Responses of the Lumbar Spine during Prolonged Stooping. *th ANNUAL MEETING*: p. 5

[23] Dakin , G.J., Arbelaez , R.A., et al. Elastic and Viscoelastic Properties of the Human Pubic Symphysis Joint: Effects of Lateral Impact Loading. *Journal of Biomechanical Engineering*, 2000. 123(3): p. 218-226

[24] Keller, T.S., Spengler, D.M., and Hansson, T.H. Mechanical behavior of the human lumbar spine. I. Creep analysis during static compressive loading. *Journal of Orthopaedic Research*, 1987. 5(4): p. 467-478

[25] Bass, C.R., Rafaels, K.A., et al. Thoracic and lumbar spinal impact tolerance. *Accident Analysis & Prevention*, 2008. 40(2): p. 487-495

[26] Wilke, H.-J., Geppert, J., and Kienle, A. Biomechanical in vitro evaluation of the complete porcine spine in comparison with data of the human spine. *European Spine Journal*, 2011. 20(11): p. 1859-1868

[27] F. McLain, R., Yerby, S.A., and Moseley, T.A. Comparative Morphometry of L4 Vertebrae: Comparison of Large Animal Models for the Human Lumbar Spine. *Spine*, 2002. 27(8): p. E200-E206

[28] Yingling, V., Callaghan, J.P., and McGill, S.M. The porcine cervical spine as a model of the human lumbar spine: an anatomical, geometric, and functional comparison. *Journal of Spinal Disorders*, 1999. 12(5): p. 415-423

[29] Callaghan, J.P. and McGill, S.M. Intervertebral disc herniation: studies on a porcine model exposed to highly repetitive ¯exion/extension motion with compressive force. *Clinical Biomechanics*, 2001
[30] Araujo, A., Peixinho, N., Pinho, A., and Claro, J.C.P. Comparison between the dynamic and initial creep response of porcine and human lumbar intervertebral discs. *Proceedings of 2015 IEEE 4th Portuguese Meeting on Bioengineering (ENBENG)*, 2015.
[31] Smit, T.H. The use of a quadruped as an in vivo model for the study of the spine – biomechanical considerations. *European Spine Journal*, 2002. 11(2): p. 137-144
[32] Nettles, D.L., Richardson, W.J., and Setton, L.A. Integrin expression in cells of the intervertebral disc. *Journal of Anatomy*, 2004. 204(6): p. 515-520
[33] Holm, S., Holm, A.K., Ekström, L., Karladani, A., and Hansson, T. Experimental Disc Degeneration Due to Endplate Injury. *Clinical Spine Surgery*, 2004. 17(1): p. 64-71
[34] Schindelin, J., Arganda-Carreras, I., et al. Fiji: an open-source platform for biological-image analysis. *Nature Methods*, 2012. 9(7): p. 676-682
[35] Thoreson, O., Baranto, A., et al. The immediate effect of repeated loading on the compressive strength of young porcine lumbar spine. *Knee Surgery, Sports Traumatology, Arthroscopy*, 2010. 18(5): p. 694-701
[36] Morino, C.F., Schmidt, A.L., et al. Human and porcine lumbar endplate injury risk in repeated flexion-compression. *Proceedings of IRCOBI*, 2023.
[37] Funk, J.R., Hall, G.W., Crandall, J.R., and Pilkey, W.D. Linear and Quasi-Linear Viscoelastic Characterization of Ankle Ligaments. *Journal of Biomechanical Engineering*, 1999. 122(1): p. 15-22
[38] Lucas, S., Bass, C., Salzar, R., Shender, B., and Paskoff, G. High-rate viscoelastic properties of human cervical spinal intervertebral discs. *Proceedings of Annual meeting of the american society of biomechanics, american society of biomechanics*, 2006.
[39] Abedi, R., Shayegan, S., Ataee, G., and Fatouraee, N. Viscoelastic modeling of ovine cervical intervertebral disc through stress-relaxation, constant strain rate and dynamic loading tests. *Proceedings of 2019 26th National and 4th International Iranian Conference on Biomedical Engineering (ICBME)*, 2019.
[40] Lakes, R., "Viscoelastic Materials". 2009: Cambridge University Press. 481.
[41] Yoganandan, N., Umale, S., Stemper, B., and Snyder, B. Fatigue responses of the human cervical spine intervertebral discs. *Journal of the mechanical behavior of biomedical materials*, 2017. 69: p. 30-38
[42] Sivasankari, S. and Balasubramanian, V. Developing a heuristic relationship to predict the spinal injury during vertical impact for autonomous vehicle and bio environment. *Computer Methods and Programs in Biomedicine*, 2020. 196: p. 105618
[43] Busscher, I., van der Veen, A.J., et al. In Vitro Biomechanical Characteristics of the Spine: A Comparison Between Human and Porcine Spinal Segments. *Spine*, 2010. 35(2): p. E35-E42

VII. APPENDIX

TABLE II
SSE and R^2 values of each model

Test Number	SSE	R^2
Test 1	4.7634	0.9968
Test 2	1.0596	0.9939
Test 3	0.5996	0.9910
Test 4	0.1037	0.9990
Test 5	0.1909	0.9984
Test 6	0.4451	0.9979
Test 7	0.5582	0.9993
Test 8	0.0036	0.9997
Test 9	0.0233	0.9997
Test 10	0.3996	0.9930
Mean	0.8147 ± 1.351	0.9969 ± 0.0030

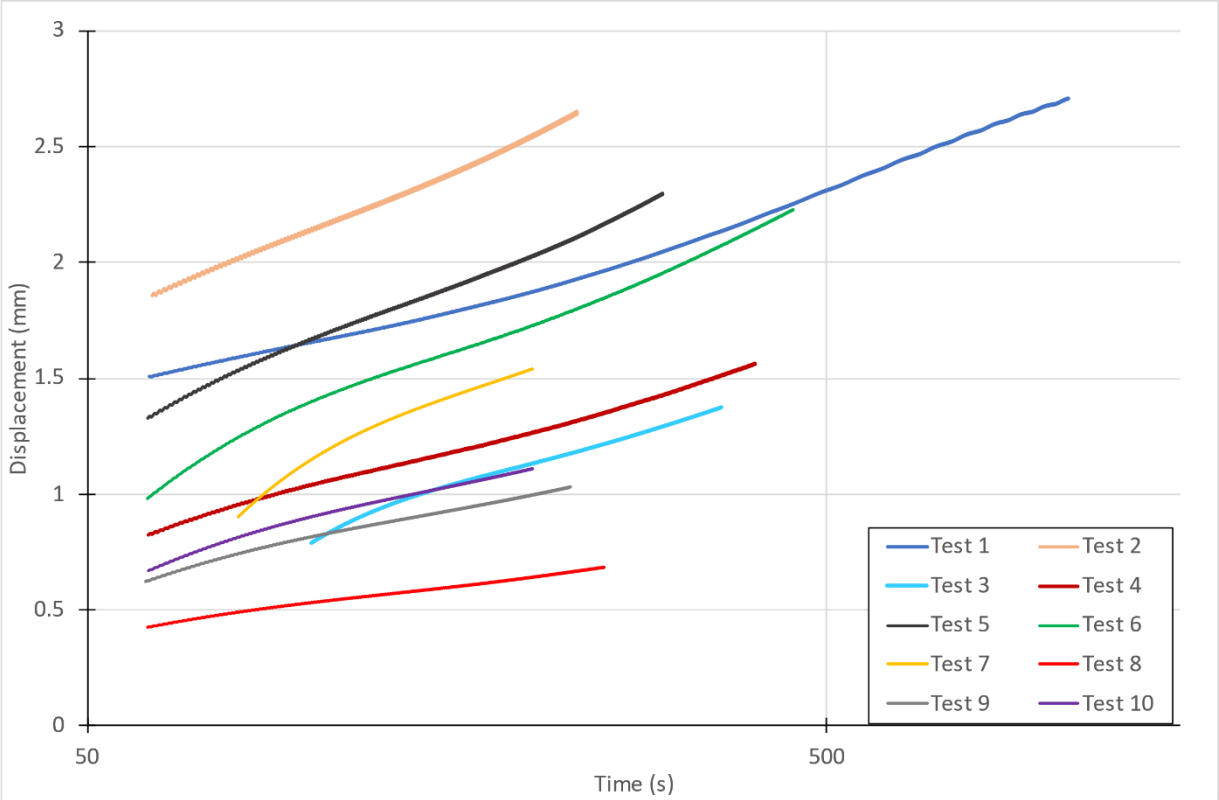

Fig. 6. Time versus model displacement for all ten models.